ChemComm

COMMUNICATION

From helix to helical pores: solid-state crystalline conversions triggered by gas–solid reactions†

Jie Liu,‡[ab] Jia-Jia Du,‡[a] Yuan Wu,[ab] Yi-Fang Zhao,[c] Xiao-Ping Zhou*[a] and Dan Li*[c]

Cite this: *Chem. Commun.*, 2017, 53, 12950

Received 27th September 2017, Accepted 8th November 2017

DOI: 10.1039/c7cc07510c

rsc.li/chemcomm

Two one-dimensional (1D) helical coordination polymers, CuBIm–Cl and CuBIm–Br (BIm = 1,2-bis((5*H*-imidazol-4-yl)-methylene)hydrazine), are constructed from Cu^{2+} ions, halides and mono-deprotonated BIm. Solid-state crystalline conversions of CuBIm–Cl and CuBIm–Br to a gyroidal metal–organic framework (MOF) STU-3 which is composed of Cu ions and Bim ligands are observed through a gas–solid reaction, where the gas is methylamine.

Metal–organic frameworks (MOFs) or porous coordination polymers (PCPs) as new-generation porous materials have received gigantic research attention due to their versatile structure and advanced applications in gas storage,[1] separation,[2] catalysis,[3] sensing,[4] medicine,[5] water harvesting,[6] *etc.* In comparison with robust zeolite porous materials, MOFs feature notable framework flexibility and solid-state reactivity owing to the non-rigid, rotatable and reversible metal–organic bonds and varied supramolecular interactions. Drastic crystal to crystal structural transformations have been observed in flexible MOFs with external stimuli,[7] which is accompanied by changes in coordination number and geometry, dimensionality, topology, interpenetration, *etc.* Such flexibility or solid-state reactivity provides additional functionalities or enhances the performance in gas storage, separation, and sensing.[7b] Structural transformation in MOFs or PCPs induced by a solvent or a coordinate guest, heating, and post-synthetic modification is well reported.[7] However, a gas–solid reaction that leads to crystal to crystal transformation in MOFs or PCPs involving a drastic structure change is still unusual. This challenge probably originates from the fact that the movement of molecules is restricted in the solid state, making the gas–solid reaction much more difficult than the solution reaction.[8]

The well-known gas–solid reactions for MOFs or PCPs are hydration reactions, in which water molecules in the air replace the coordinated ligands and decompose the frameworks or transform them into less porous MOFs. For example, Long *et al.* reported that the famous MOF-5 is sensitive to moisture and converts into non-porous MOF-69c in air.[9] We previously reported a three dimensional (3D) Cu MOF based on a triazole ligand that can be transformed into a zero dimensional (0D) monomer complex by exposing it to air for one month.[10] Similarly, Zhang *et al.* showed that a 4-fold interpenetrated diamondoid MOF $[Cu(tzbc)_2]$ (Htzbc = 4-(1*H*-1,2,4-triazol-1-yl)benzoic acid) can be transformed into a 0D monomer $[Cu(tzbc)_2 4H_2O]$ by exposing it to air at room temperature for three months.[11] On the other hand, crystals of a nonporous coordination polymer have been reported to also show crystalline solid transformation through a chemical reaction with a gas. For example, some nonporous coordination polymers/complexes based on pyridine or imidazole ligands can undergo a reaction with hydrated HCl vapour leading to the formation of crystalline hydrogen-bonded salts.[12] Leznoff *et al.* reported that 3D coordination polymers $Zn[Au(CN)_2]_2$ react with NH_3 vapor in a stepwise manner to obtain 1D $\{Zn(NH_3)_2[Au(CN)_2]_2\}$ and probably a 0D coordination complex $Zn(NH_3)_4[Au(CN)_2]_2$.[13] In the above mentioned MOF examples, the gas–solid reactions destroy the porosity or framework structures, consequently, resulting in the loss of certain functions (*e.g.* gas adsorption).

Herein, we report a solid-state crystalline conversion from one-dimensional (1D) coordination polymers based on copper halide and a bis-imidaozole ligand, containing two types of helices with opposite chirality as an internal racemate, to a three-dimensional (3D) porous supramolecular network featuring a gyroidal surface with **gie** topology in the presence of gaseous methylamine (Scheme 1). The unusual crystal to crystalline powder transformation accompanies breaking and making of covalent bonds, dative bonds and hydrogen bonds, changing the dimensionality (1D to 3D), yielding a gyroidal surface, and generating porosity. The reaction of a basic gas with a

[a] *Department of Chemistry, Shantou University, Guangdong 515063, P. R. China. E-mail: zhouxp@stu.edu.cn*

[b] *Department of Chemistry and State Key Laboratory of Synthetic Chemistry, The University of Hong Kong, Pokfulam Road, Hong Kong, P. R. China*

[c] *College of Chemistry and Materials Science, Jinan University, Guangzhou 510632, P. R. China. E-mail: danli@jnu.edu.cn*

† Electronic supplementary information (ESI) available: Experimental section, characterization and physical measurements. CCDC 1565656 and 1565655. For ESI and crystallographic data in CIF or other electronic format see DOI: 10.1039/c7cc07510c

‡ These authors contributed equally.

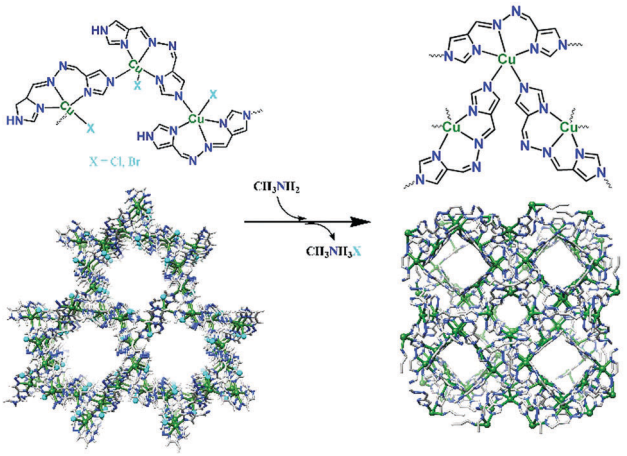

Scheme 1 Schematic representation of solid-state conversion of helical coordination polymers CuBIm–X (X = Cl, Br) to Gyroidal MOF STU-3 triggered by gaseous methylamine.

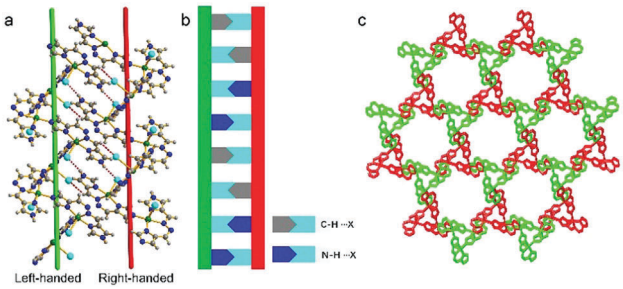

Fig. 1 View of the assembly of the adjacent two helical chains through X–H···Cl hydrogen bonds (X = C, N) in CuBIm–Cl (a, red dashed lines highlighting the hydrogen bonds), the cartoon of the assembly of two chains (b), and 3D supramolecular network showing the 1D channels through assembly of the *M* and *P* helices along the *c* axis (c, *M* helix green, *P* helix red). Color codes: Cu green, Cl cyan, C gray, H light gray, and N blue.

coordination polymer to induce a crystal to crystalline powder transformation to a 3D MOF is observed for the first time to the best of our knowledge.

Coordination polymers CuBIm–Cl and CuBIm–Br (BIm = 1,2-bis((5*H*-imidazol-4-yl)-methylene)hydrazine) were synthesized by reacting ligand BIm with the respective copper halide salts under solvothermal conditions, where BIm was conveniently obtained by the condensation of hydrazine monohydrate and 4-formylimidazole in methanol following the procedure given in previous work.[14] Dark green needle-like crystals of CuBIm–Cl and CuBIm–Br were collected by heating a mixture of CuX_2 (X = Cl^- and Br^-) and BIm in 4 : 1 (v/v) *N*,*N*-dimethylformamide (DMF)/ethanol at 100 °C in sealed Pyrex glass tubes for three days (see the ESI† for details). The purity of CuBIm–Cl and CuBIm–Br is documented by both powder X-ray diffraction studies (Fig. S1, ESI†) and CHN elemental analyses.

Single-crystal X-ray diffraction (SCXRD) studies revealed that both CuBIm–Cl and CuBIm–Br crystallize in the trigonal space group $R\bar{3}$ and adopt an identical 1D extended helix structure. As an example, the structure of CuBIm–Cl will be described in detail. As shown in Fig. S2a (ESI†), the asymmetric unit of CuBIm–Cl contains one BIm ligand, one Cu(II) ion, and one Cl^- anion. The Cu(II) center is five-coordinated and adopts a distorted square pyramidal geometry, by binding 4 nitrogen atoms and a chloride anion (Fig. S2c, ESI†), and the +2 positive charge is balanced by one mono-deprotonated BIm and Cl^-. The Cu–Cl bond distance (2.5884(7) Å) is elongated compared to that of a normal Cu–Cl bond due to the Jahn–Teller effect. The mono-deprotonated BIm bridging the Cu(II) forms an extended 3_1 helical chain along the *c* axis with a pitch of 9.713 Å. It is worth noting that there exist two types of helices featuring opposite chirality (left-handed (*M*) and right-handed (*P*)) (Fig. S2b, ESI†), which lead to racemic packing and achiral crystals. The coordination chemistry of multimodal ligand BIm is similar to that of the multimodal ligands that are used in previous studies.[15]

As shown in Fig. 1a and Fig. S2c (ESI†), left-handed and right-handed helices assemble together tightly, and multi-type supramolecular interactions (N–H···Cl, C–H···Cl, and π···π) exist between the two adjacent helices. The π···π interaction distance is about 3.630 Å, and the hydrogen bonds are N···Cl = 3.092 Å, and C···Cl = 3.413 Å, respectively. It should be noted that the stretching vibrations of N–H shift to lower wavenumbers (3117 cm^{-1}) in the IR spectrum in comparison with about 3300 cm^{-1} of normal N–H shift in imidazole, which is probably caused by the N–H···Cl hydrogen bonds (Fig. S3, ESI†). The synergy of multi-type supramolecular interactions between the left-handed and right-handed helices is similar to DNA assembly, as shown in Fig. 1a and b. Each helix assembles with three opposite chiral helices in parallel. A 3D porous supramolecular network is constructed, which has 1D infinite nano-hexagonal channels along the *c*-axis (Fig. 1c) with a pore aperture of 6.815 Å for CuBIm–Cl and 8.124 Å for CuBIm–Br, respectively (Fig. S4, ESI†). The total potential solvent area volumes for CuBIm–Cl and CuBIm–Br are 2226.9 $Å^3$ (33.9%) and 2289.83 $Å^3$ (33.8%) in one unit cell, respectively, checked using the PLATON program. The self-assembly of left-handed and right-handed helices to afford a porous supramolecular network is very scarce in reported supramolecular porous materials, although the packing of the 1D chain to form a porous structure has been well reported.[16]

Porous CuBIm–Cl and CuBIm–Br are highly stable in air. Crystals of both compounds maintain good crystallinity upon exposure to air for 3 months. TGA studies show that they can remain stable at a high temperature of up to 280 °C under a N_2 atmosphere (Fig. S5, ESI†). Moreover, testified by variable-temperature powder X-ray diffraction (Fig. S6, ESI†), CuBIm–Cl and CuBIm–Br are found to maintain crystallinity at high temperatures of up to 275 °C and 325 °C in air, which is slightly different from the TGA results and probably due to the different gas environments. Their chemical stability in boiling water and organic solvents was also explored. The PXRD study for the treated samples showed that CuBIm–Cl and CuBIm–Br are stable in boiling THF and benzene for 24 hours (Fig. S7, ESI†), whereas they are not stable in water. An unknown phase is found after being treated in boiling water for 24 hours (Fig. S8, ESI†).

Although both CuBIm–Cl and CuBIm–Br are stable under heating conditions and in boiling THF and benzene, the elongated Cu–Cl/Br bonds (Cu–Cl 2.5884(7) Å, Cu–Br 2.7430(5) Å) and short H···Cl distances (2.233 Å) give a clue that they probably can react with basic gas through an acid–base reaction. Crystalline samples of CuBIm–Cl and CuBIm–Br (10.0 mg) placed in a small opened

vial were exposed to an atmosphere of methylamine (1.0 mL methylamine in an ethanol solution, 33 wt%) in a large sealed vessel. Due to the existence of channels, methylamine vapors are expected to diffuse into solid CuBIm–Cl and CuBIm–Br and to react with Cl^-/Br^- and mono-deprotonated BIm forming methylammonium chloride/bromine. A colour change from dark green to light-green was observed within half an hour for both samples (Fig. S9, ESI†), which is probably caused by further deprotonation of the mono-deprotonated Bim and modification of the geometry around the Cu centres. Both single crystal samples are broken and changed to powders after the gas–solid reactions, and their structures cannot be determined by SCXRD technology. Fortunately, the resulting solids are still crystalline. PXRD studies show that the patterns are in accordance with that of our previously reported MOF STU-3 (Fig. S10, ESI†).[14] To confirm that the PXRD is identical to that of STU-3, we performed Pawley refinements (Fig. S11, ESI†). The resulting unit cell parameters obtained by refinement are in good accordance with those of STU-3 obtained by SCXRD (Table S2, ESI†), suggesting that the 1D polymers have transformed into STU-3. The structure of STU-3 is composed of Cu(II) ions and fully deprotonated BIm ligands and features a gyroidal surface with **gie** topology (identical with BSV zeolite)[17] and helical pores. Postsynthetic structural modification to prepare MOF materials has been well demonstrated recently,[18] including the use of 1D polymers to make 3D MOFs.[18d,e]

To understand the details of the crystal to crystal transformation, we monitored the process by time-resolved PXRD (Fig. 2 and Fig. S12, ESI†). At the early stage of the reaction, the peaks of 2theta-angles slightly shift to higher angles (*e.g.* 6.0 to 6.3 degrees for CuBIm–Cl). This shift is probably because of the framework shrink caused by gaseous absorption of methylamine. Then, the peak intensities of the shrunken frameworks reduce gradually, while the peaks belonging to STU-3 arise and become distinct with the lapse of time. Finally, after about half an hour, CuBIm–Cl or CuBIm–Br transform into STU-3 successfully in a quantitative, crystalline-state reaction. The PXRD pattern of the product that transformed from CuBIm–Br after exposure to methylamine for 60 minutes is broader than that of CuBIm–Cl, which is probably due to the relatively poor crystallinity after the transformation. Besides the framework shrink, there is no other immediate phase observed during the transformation. The drastic changes after crystal transformation for CuBIm–Cl and CuBIm–Br in comparison with STU-3 include: (i) the crystal lattice transformation from hexagonal $R\bar{3}$ to highest symmetric cubic $Ia\bar{3}d$; (ii) the Cu–Cl/Br dative bonds, N–H covalent bonds, N–H···Cl/Br and C–H···Cl/Br hydrogen bonds, and π···π interactions are broken and the new Cu–N dative bonds, N–H covalent bonds, and $Cl^-/Br^-\cdots CH_3NH_3^+$ ionic interactions are formed; (iii) the solvent-accessible volume per unit cell increases from 34.5%–36.6% to 50.4%; (iv) CuBIm helices need a drastic rearrangement to generate the unusual gyroidal surface and **gie** topological linkage, and N atoms of a new deprotonated imidazole group need to move at least 2.1 Å to bind with the closest Cu(II) centers.

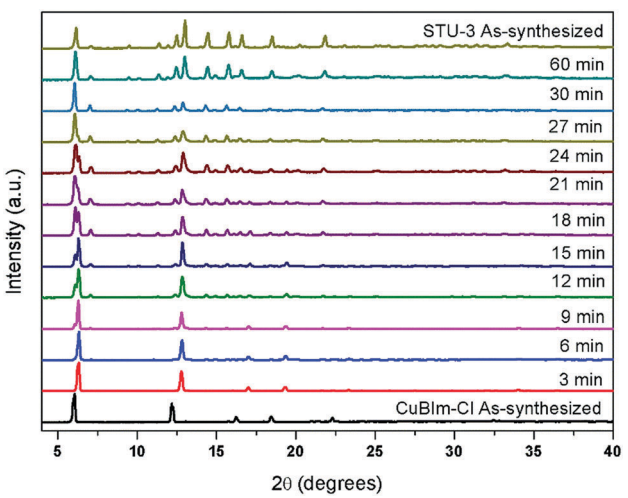

Fig. 2 Time-resolved X-ray powder diffractions monitoring the transformation of crystalline CuBIm–Cl into STU-3 under a methylamine atmosphere.

The detail mechanism of solid transformation from CuBIm–Cl and CuBIm–Br into STU-3 is still unclear. A possible reason is that both CuBIm–Cl and CuBIm–Br are intermediate states of STU-3. Notably, both products of needle crystals of CuBIm–Cl or CuBIm–Br and block crystals of STU-3 were observed in the reactions (Fig. S13, ESI†), when the temperature of synthesis increases to 120 °C. This result shows that the high temperature is in favor of forming STU-3, suggesting that STU-3 is a thermodynamic product and CuBIm–Cl or CuBIm–Br is a kinetic product. Therefore, both CuBIm–Cl and CuBIm–Br spontaneously transform into STU-3 when basic methylamine gas is present and reacts with them.

In order to further prove the transformation process, we carried out IR spectra measurements (Fig. S14, ESI†), thermal gravimetric analysis (Fig. S15, ESI†), and CHN elemental analysis (Table S3, ESI†). These measurement results are in good accordance with that of STU-3 obtained from direct synthesis, providing unequivocal evidence for the successful transformation. To check if the Cl^- and Br^- ions were removed from the coordination polymers successfully after reacting with gaseous methylamine, we soaked the transformed polycrystalline sample in methanol to exchange with the yielded methylammonium chloride/bromine. Upon treating the supernatant of the mixture with Ag^+, white AgCl and light-yellow AgBr precipitates were formed immediately (Fig. S16, ESI†), respectively, indicating that Cl^- and Br^- anions were dissolved in methanol solution accompanied by methylammonium. Further studies of energy dispersive X-ray (EDX) analysis show that there are very few Cl^- or Br^- ions present in the transformed products, which were exchanged and washed with methanol (Fig. S17 and S18, ESI†). We also considered whether gyroidal STU-3 can be transformed back to CuBIm–Cl and CuBIm–Br by exposing to a HCl and HBr vapour, respectively. Unfortunately, after being exposed to HCl for 1 hour, STU-3 showed an unknown phase in the PXRD pattern (Fig. S19, ESI†), while there was no change when exposed to HBr atmosphere. The preliminary studies indicate that the transformations between helical coordination polymers (CuBIm–Cl and CuBIm–Br) and gyroidal MOF STU-3 are not reversible.

To evaluate the permanent porosity of CuBIm–Cl, CuBIm–Br and their transformed STU-3 products through gas–solid

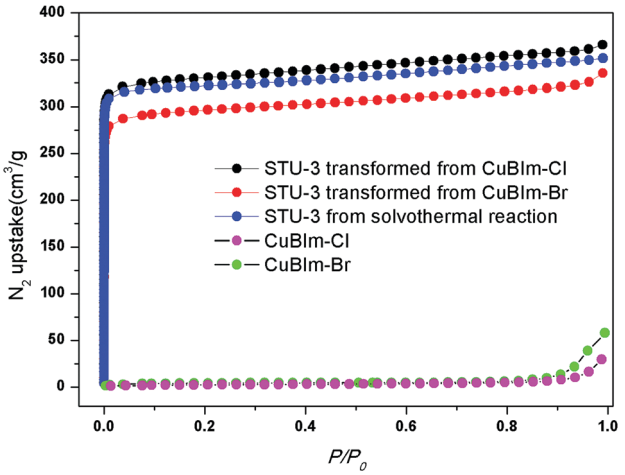

Fig. 3 N_2 adsorption isotherm of CuBIm–Cl, CuBIm–Br, STU-3 from the solvothermal reaction, and STU-3 transformed from CuBIm–Cl and CuBIm–Br, respectively.

reactions, N_2 gas adsorption measurements at 77 K were performed (Fig. 3). Although both CuBIm–Cl and CuBIm–Br are thermally stable and show a distinctive void volume (36.6% for CuBIm–Cl, 34.5% for CuBIm–Br), the N_2 adsorption measurements show that very little N_2 is taken up at low pressure and give very low Brunauer–Emmett–Teller (BET, 8 and 9 $m^2\ g^{-1}$, respectively) and Langmuir surface areas (14 and 17 $m^2\ g^{-1}$, respectively). The experimental surface areas are very different from the theoretically calculated results (1224 $m^2\ g^{-1}$ for CuBIm–Cl, and 1035 $m^2\ g^{-1}$ for CuBIm–Br). This high disagreement was probably caused by a loss of structural integrity upon desolvation (Fig. S20, ESI†), significantly reducing the porosity and surface areas.[19] However, transformed from CuBIm–Cl and CuBIm–Br *via* gas–solid reactions, the products can adsorb 364 $cm^3\ g^{-1}$ and 334 $cm^3\ g^{-1}$ N_2, under 77 K and P/P_0 = 0.99, respectively, and exhibit type I adsorption isotherms as typical microporous materials. The BET and Langmuir surface areas are calculated to be 995 and 890 $m^2\ g^{-1}$, and 1417 and 1267 $m^2\ g^{-1}$, respectively, which are comparable to those of STU-3 synthesized by a solvothermal method (963 and 1422 $m^2\ g^{-1}$, respectively). The slightly lower N_2 uptake of the product that was transformed from CuBIm–Br is probably due to its relatively poor crystalline property when compared to that of CuBIm–Cl.

To conclude, we have demonstrated an unusual crystal to crystal transformation triggered by a gas–solid reaction. In the process, helical CuBIm–Cl and CuBIm–Br coordination polymers transform into gyroidal MOF STU-3, due to the fact that methylamine reacts with hydrogen bonded H···Cl/Br (with Cu center) yielding methylammonium chloride/bromine. This crystalline conversion represents a unique example of transformation from low porous coordination polymers to microporous materials induced by gas–solid reactions, providing a new route to discover novel, and useful structural rearrangements of MOF materials in the future.

This work is financially supported by the National Basic Research Program of China (973 Program 2013CB834803), the National Natural Science Foundation of China (21731002, 91222202, 21171114, 21371113), Guangdong Natural Science Funds for Distinguished Young Scholars (2014A030306042), and the Training Program for Excellent Young College Teacher of Guangdong Province.

Conflicts of interest

There are no conflicts to declare.

Notes and references

1 (*a*) B. Li, H.-M. Wen, W. Zhou, J. Q. Xu and B. Chen, *Chemistry*, 2016, **1**, 557; (*b*) L. J. Murray, M. Dinca and J. R. Long, *Chem. Soc. Rev.*, 2009, **38**, 1294.
2 J.-R. Li, J. Sculley and H.-C. Zhou, *Chem. Rev.*, 2012, **112**, 869.
3 M. Yoon, R. Srirambalaji and K. Kim, *Chem. Rev.*, 2012, **112**, 1196.
4 (*a*) L. E. Kreno, K. Leong, O. K. Farha, M. Allendorf, R. P. Van Duyne and J. T. Hupp, *Chem. Rev.*, 2012, **112**, 1105; (*b*) Y. Cui, Y. Yue, G. Qian and B. Chen, *Chem. Rev.*, 2012, **112**, 1126.
5 (*a*) J. Della Rocca, D. Liu and W. Lin, *Acc. Chem. Res.*, 2011, **44**, 957; (*b*) P. Horcajada, T. Chalati, C. Serre, B. Gillet, C. Sebrie, T. Baati, J. F. Eubank, D. Heurtaux, P. Clayette, C. Kreuz, J.-S. Chang, Y. K. Hwang, V. Marsaud, P.-N. Bories, L. Cynober, S. Gil, G. Ferey, P. Couvreur and R. Gref, *Nat. Mater.*, 2010, **9**, 172.
6 H. Kim, S. Yang, S. R. Rao, S. Narayanan, E. A. Kapustin, H. Furukawa, A. S. Umans, O. M. Yaghi and E. N. Wang, *Science*, 2017, **356**, 430.
7 (*a*) S. Kitagawa, R. Kitaura and S.-I. Noro, *Angew. Chem., Int. Ed.*, 2004, **43**, 2334; (*b*) Z. Chang, D.-H. Yang, J. Xu, T.-L. Hu and X.-H. Bu, *Adv. Mater.*, 2015, **27**, 5432; (*c*) J.-P. Zhang, P.-Q. Liao, H.-L. Zhou, R.-B. Lin and X.-M. Chen, *Chem. Soc. Rev.*, 2014, **43**, 5789; (*d*) A. Schneemann, V. Bon, I. Schwedler, I. Senkovska, S. Kaskel and R. A. Fischer, *Chem. Soc. Rev.*, 2014, **43**, 6062; (*e*) G. K. Kole and J. J. Vittal, *Chem. Soc. Rev.*, 2013, **42**, 1755; (*f*) G. Ferey, *New J. Chem.*, 2016, **40**, 3950.
8 J. J. Vittal and H. S. Quah, *Coord. Chem. Rev.*, 2017, **342**, 1.
9 S. S. Kaye, A. Dailly, O. M. Yaghi and J. R. Long, *J. Am. Chem. Soc.*, 2007, **129**, 14176.
10 D. Liu, M. Li and D. Li, *Chem. Commun.*, 2009, 6943.
11 M.-M. Liu, Y.-L. Bi, Q.-Q. Dang and X.-M. Zhang, *Dalton Trans.*, 2015, **44**, 19796.
12 (*a*) E. Coronado, M. Giménez-Marqués, G. M. Espallargas and L. Brammer, *Nat. Commun.*, 2012, **3**, 828; (*b*) C. J. Adams, M. F. Haddow, M. Lusi and A. G. Orpen, *Proc. Natl. Acad. Sci. U. S. A.*, 2010, **107**, 16033; (*c*) C. J. Adams, H. M. Colquhoun, P. C. Crawford, M. Lusi and A. G. Orpen, *Angew. Chem., Int. Ed.*, 2007, **46**, 1124; (*d*) S. M. Fellows and T. J. Prior, *Cryst. Growth Des.*, 2017, **17**, 106; (*e*) G. Mínguez Espallargas, M. Hippler, A. J. Florence, P. Fernandes, J. van de Streek, M. Brunelli, W. I. F. David, K. Shankland and L. Brammer, *J. Am. Chem. Soc.*, 2007, **129**, 15606.
13 M. J. Katz, T. Ramnial, H.-Z. Yu and D. B. Leznoff, *J. Am. Chem. Soc.*, 2008, **130**, 10662.
14 X.-P. Zhou, M. Li, J. Liu and D. Li, *J. Am. Chem. Soc.*, 2012, **134**, 67.
15 (*a*) N. S. Oxtoby, A. J. Blake, N. R. Champness and C. Wilson, *Proc. Natl. Acad. Sci. U. S. A.*, 2002, **99**, 4905; (*b*) A. J. Blake, N. R. Champness, P. A. Cooke, J. E. B. Nicolson and C. Wilson, *J. Chem. Soc., Dalton Trans.*, 2000, 3811; (*c*) A. J. Blake, N. R. Champness, P. A. Cooke and J. E. B. Nicolson, *Chem. Commun.*, 2000, 665.
16 W. L. Leong and J. J. Vittal, *Chem. Rev.*, 2011, **111**, 688.
17 T. E. Gier, X. Bu, P. Feng and G. D. Stucky, *Nature*, 1998, **395**, 154.
18 (*a*) J.-H. Wang, Y. Zhang, M. Li, S. Yan, D. Li and X.-M. Zhang, *Angew. Chem., Int. Ed.*, 2017, **56**, 6478; (*b*) C.-P. Li, H. Zhou, Y. Ju and M. Du, *Chem. – Eur. J.*, 2017, **23**, 12985; (*c*) C.-X. Chen, Z.-W. Wei, J.-J. Jiang, S.-P. Zheng, H.-P. Wang, Q.-F. Qiu, C.-C. Cao, D. Fenske and C.-Y. Su, *J. Am. Chem. Soc.*, 2017, **139**, 6034; (*d*) D. Kim and A. Coskun, *Angew. Chem., Int. Ed.*, 2017, **56**, 5071; (*e*) P. A. Julien, K. Užarević, A. D. Katsenis, S. A. J. Kimber, T. Wang, O. K. Farha, Y. Zhang, J. Casaban, L. S. Germann, M. Etter, R. E. Dinnebier, S. L. James, I. Halasz and T. Friščić, *J. Am. Chem. Soc.*, 2016, **138**, 2929.
19 O. K. Farha and J. T. Hupp, *Acc. Chem. Res.*, 2010, **43**, 1166.